Accepted Manuscript

Microstructural and textural characteristics of soy protein isolate and tara gum cold-set gels

Romina Ingrassia, Lucas L. Bea, María E. Hidalgo, Patricia H. Risso

PII: S0023-6438(19)30626-7

DOI: https://doi.org/10.1016/j.lwt.2019.108286

Article Number: 108286

Reference: YFSTL 108286

To appear in: *LWT - Food Science and Technology*

Received Date: 9 May 2019

Revised Date: 11 June 2019

Accepted Date: 18 June 2019

Please cite this article as: Ingrassia, R., Bea, L.L., Hidalgo, Marí.E., Risso, P.H., Microstructural and textural characteristics of soy protein isolate and tara gum cold-set gels, *LWT - Food Science and Technology* (2019), doi: https://doi.org/10.1016/j.lwt.2019.108286.

This is a PDF file of an unedited manuscript that has been accepted for publication. As a service to our customers we are providing this early version of the manuscript. The manuscript will undergo copyediting, typesetting, and review of the resulting proof before it is published in its final form. Please note that during the production process errors may be discovered which could affect the content, and all legal disclaimers that apply to the journal pertain.

ACCEPTED MANUSCRIPT

Microstructural and textural characteristics of soy protein isolate and tara gum cold-set gels

Romina Ingrassia[a,b,c,*], Lucas L. Bea[a], María E. Hidalgo[a,b], Patricia H. Risso[a,b,c]

[a] Facultad de Ciencias Bioquímicas y Farmacéuticas, Universidad Nacional de Rosario (UNR), Suipacha 531, S2002LRK Rosario, Santa Fe, Argentina

[b] Consejo Nacional de Investigaciones Científicas y Técnicas (CONICET), Godoy Cruz 2290, C1425FQB CABA, Buenos Aires, Argentina

[c] Facultad de Ciencias Veterinarias, UNR, Ovidio Lagos y Ruta 33, 2170 Casilda, Santa Fe, Argentina

* Corresponding author

Dra. Romina Ingrassia

Facultad de Ciencias Bioquímicas y Farmacéuticas. Universidad Nacional de Rosario Suipacha 531. S2002RLK Rosario. Argentina.

E-mail: romina_ingrassia@yahoo.com.ar

ACCEPTED MANUSCRIPT

ACCEPTED MANUSCRIPT

Abstract

Soy protein isolates (SPI) are capable of forming cold-set gels. This techno-functional property can be affected by the presence of tara gum (TG). Under certain conditions, these SPI/TG systems may also form water-in-water (W/W) emulsions. The aim of this study was to evaluate acid gels formed from soy protein isolates (SPI) and tara gum (TG) aqueous mixtures, and to find the conditions in which the W/W emulsions of SPI droplets dispersed in a TG continuous phase can be stabilized by SPI gelation as a strategy to prevent emulsion destabilization. Cold-set gels of SPI 0.3g/L at different TG concentrations (0-0.05g/L) showed different microstructures, a consequence of a different balance between gelation and segregative phase separation processes. SPI gels showed a homogenous and compact microstructure. When TG was present at 0.01g/L and 0.02g/L, the protein network was less interconnected, showing coarse-stranded and bicontinuous gels, respectively. At TG>0.03g/L, stable W/W emulsions were formed, revealing an abrupt decrease in gel firmness, a significant loss of fracture capacity, and a decrease in the water holding capacity. These findings may be used as a starting point for the application of these gelled systems as thickeners, texture modifiers, and coating materials for delivery of bioactive compounds.

KEYWORDS: thermodynamic compatibility; cold-set gelation; confocal microscopy; water holding capacity; water-in-water emulsions

ACCEPTED MANUSCRIPT

ACCEPTED MANUSCRIPT

1. Introduction

Protein gelation is an important functional property as it has a key role during the preparation of a wide range of products. In recent years, the gelation of globular proteins at room temperature, known as "cold gelation", has gained interest. This process consists of two consecutive stages. In the first one, protein aggregates are formed by heating the protein solution at a pH far from the isoelectric point and, after cooling, these aggregates remain soluble. In the second stage, gelation is induced by the addition of salts or by a decrease in pH (Alting, de Jongh, Visschers, & Simons, 2002). The pH reduction of protein solutions may be performed by adding glucono-δ-lactone (GDL), which is hydrolyzed in aqueous solution, releasing gluconic acid. The rate of pH reduction depends on the concentration of GDL and the temperature (de Kruif, 1997).

Soy protein isolates (SPI) has been reported to be capable of forming acid gels after thermal denaturation and acidification up to a pH close to the isoelectric point of its main proteins. This behavior has been studied as a starting point for the preparation of tofu-like products (Campbell, Gu, Dewar, & Euston, 2009; Gu, Campbell, & Euston, 2009).

On the other hand, the protein gelation process can be affected by the presence of polysaccharides due to the possible existence of thermodynamic incompatibility between both biopolymers (Grinberg & Tolstoguzov, 1997; Tolstoguzov, 2003). Thermodynamic incompatibility may involve a charged protein and a similarly charged or neutral polysaccharide (Doublier, Garnier, Renard, & Sanchez, 2000). This phenomenon may be accompanied by the gelation of one of the biopolymers. Thus, depending on the balance between the rate of gelation and phase separation processes, the final gel microstructure obtained will vary (Corredig, Sharafbafi, & Kristo, 2011; Kasapis, 2008; Tavares, Monteiro, Moreno, & Lopes da Silva, 2005).

In the absence of gelation, thermodynamic incompatibility leads to a segregative phase separation in which each phase is enriched in one of the two biopolymers (Corredig et al., 2011; Stieger & van de Velde, 2013). In these aqueous two-phase systems, water-in-water (W/W) emulsions may be formed by dispersing an aqueous solution into another aqueous phase, i.e. as droplets of one biopolymer distributed in a continuous phase of the other biopolymer (Esquena, 2016; Norton & Frith, 2001). The main problem with W/W emulsions is their usual lack of kinetic stability, since they tend to coalesce or flocculate quickly. Lundin et al. (1999) have reported that if one or both of the biopolymers gelify, stable W/W emulsions can be obtained by controlling the thermal gelation rate due to the formation of gelled states. Khan, Nickerson, Paulson, Rousseau & Dérick (2011) have also reported that it can be possible to generate hydrogel microstructures via phase separation of thermodynamically incompatible binary biopolymer mixtures. In a more recent study, Esquena (2016) postulated that it would be possible to obtain stable W/W emulsions by the formation of gelled states that prevented coalescence and that these W/W emulsions could be used as templates for the formation of microgels.

Tara gum (TG) is a galactomannan obtained from the seeds of *Caesalpinia spinosa.* It consists of a skeleton of (1→4)-linked β-D-mannopyranosyl sugar units, one-third of which are (1→6)-linked with α-D-galactopyranosyl as side groups (Anderson, 1949; Buffington, Stevens, Morris, & Rees, 1980). In recent years, reports on the use of TG as a food additive have been increasing due to its ability to act as a stabilizing agent, emulsifier and thickener, and to avoid undesirable effects in gelled products like syneresis (Daas, Grolle, van Vliet, Schols, & de Jongh, 2002; Jóźwiak, Dziubiński, & Orczykowska, 2018; Singh, Singh, & Arya, 2018; Wu, Ding, & He, 2018). TG is also used in the preparation of sustained and immediate release formulations because it is a

swelling agent, a binder and a mucoadhesive with sustained effect (Ananthakumar, Chitra, & Satheshkumar, 2018; Goswami & Naik, 2014).

On the other hand, consumption of soy protein-based food products is increasing not only because of its reported beneficial effects on nutrition and health but also due to increased concerns about the safety of animal-derived products and to the relatively high abundance of the raw material, which is a byproduct of the industrial soy oil processing (Friedman & Brandon, 2001; Moure, Sineiro, Domínguez, & Parajó, 2006; Xiao, 2011).

Despite the potential applications of SPI and TG in food systems as described above, as far as we know, there has been reported only one study of SPI/TG gelled systems. Monteiro, Rebelo, da Cruz e Silva & Lopes-da-Silva (2013) studied SPI/TG heat-induced gels with microstructures that strongly depended on both biopolymer concentrations. However, under the conditions evaluated, these authors did not obtain colloidal dispersions of protein microgel particles (droplets-like) in a polysaccharide-rich phase.

The aim of the present study was to evaluate acid gels formed from SPI/TG aqueous mixtures and to find the conditions in which the W/W emulsions are stabilized by cold-set gelation as a strategy to prevent emulsion destabilization. The results obtained may be useful for further applications of these gelled systems as thickeners, texture modifiers, and coating materials for delivery of bioactive compounds.

2. Materials and methods

2.1. Materials and sample preparation

The soy protein isolate (SPI) was prepared following the procedures detailed by Sorgentini & Wagner (1999) with some modifications. First, active defatted soy flour

ACCEPTED MANUSCRIPT

without thermal inactivation of anti-nutritional factors (Molinos Río de la Plata, Argentina) was milled and sequentially passed through 590-µm and 297-µm sieves. Later, 50 g of this soy flour was added and stirred in 500 mL of distilled water for 2 h, keeping the pH at 8.0 with a 2 mol/L NaOH (Cicarelli, Argentina). The dispersion was centrifuged at 10,400 g for 20 min at 20 °C and the precipitate was discarded. The supernatant was acidified to pH 4.5 with 1 mol/L HCl (Cicarelli, Argentina) causing the precipitation of soy storage proteins. The precipitate was left overnight in contact with the supernatant and then washed with a dilute solution of HCl (pH 4.5) to remove salts. Centrifugation was repeated at 10,400 g for 20 min at 20 °C. The precipitate was solubilized by taking the pH to 8 with 2 N NaOH and freeze-dried. The protein content of SPI was determined according to the Micro Kjeldahl method (N×6.25) (Nkonge & Ballance, 1982) and resulted to be (92 ± 2)%.

Tara gum (TG) was provided by G&G Suministros (Rosario, Argentina). Rhodamine B and glucono-δ-lactone (GDL) were purchased from Sigma-Aldrich Co. (Steinheim, Germany).

TG and SPI stock solutions (0.1 g/L and 0.9 g/L, respectively) were prepared by dissolving the corresponding powders in distilled water or buffer phosphate 10 mmol/l pH 7 under magnetic stirring at room temperature. Binary solutions of SPI/TG were prepared by mixing weighted amounts of TG and SPI stock solutions and distilled water or buffer phosphate 10 mmol/L pH 7.0 at 25 ºC.

2.2. Phase diagram

In order to evaluate the existence of thermodynamic incompatibility between the biopolymers, phase diagrams of mixtures in different proportions of TG and SPI were made, and the visual inspection was carried out after an incubation period (Spyropoulos,

Portsch, & Norton, 2010). If one or both biopolymers are highly viscous or form gels, the rate and extent of phase separation can be significantly delayed. Therefore, to avoid misleading interpretations these biopolymer mixtures must be incubated for a relatively longer period than the experimental one to ensure whether phase separation occurs (Stieger & van de Velde, 2013).

Binary systems were prepared by mixing stock solutions of SPI, TG, and buffer phosphate 10 mmol/L pH 7 in order to achieve a final concentration of SPI and TG ranging from 0.05 to 0.5 g/L and 0.005 to 0.04 g/L, respectively. The systems were then incubated for 48 h at 25 °C.

2.3. SPI acid gelation

As a first step for cold-set gelation, protein denaturation was promoted by heating 0.6 g/L SPI stock solution prepared in distilled water at 100ºC for 5 min. Immediately after this heat treatment, the dispersion was cooled in an ice-water bath to avoid further protein aggregation and precipitation. Then, SPI and SPI/TG systems were prepared by mixing this heat-treated SPI stock solution, TG stock solution (0.1 g/L), and distilled water in order to achieve a final SPI concentration of 0.3 g/L and a final TG concentration ranging from 0 to 0.05 g/L. As a second and final step, protein acid gelation was induced by the addition of solid GDL. GDL hydrolysis promotes a pH decrease at a rate that depends on the GDL concentration and the temperature (de Kruif, 1997). Protein acid gelation at 25 °C was initiated by the addition of solid GDL to SPI solutions in the presence and absence of TG (0-0.05 g/L). The amount of GDL added was enough to achieve a final concentration of 0.15 g/L.

In order to study the effect of the presence of TG on the surface charge of heat-treated SPI proteins (100ºC, 5 min), the electrokinetic potential (ζ) of SPI and SPI/TG

dispersions (0.3 g/L SPI and 0, 0.01, 0.03, 0.05 g/L TG) were determined in a Nano Particle Analyzer Horiba SZ-100 (Kyoto, Japan). Aqueous solutions were filtered through a Minisart® Syringe filter (Sartorius Stedim Biotech GmbH, Goellingen, Germany) with a cut-off of 0.2 μm (Anema & Klostermeyer, 1996).

2.4. Gel microstructure analysis

SPI/TG gel microstructure was studied by confocal laser scanning microscopy (CLSM). SPI solutions (0.3 g/L) and SPI/TG solutions (0.01, 0.02, 0.03, 0.04, and 0.05 g/L/0.3 g/L, respectively) were stained with a small aliquot of Rhodamine B solution (0.05 g/L) in a proportion of 66 μg Rhodamine per g protein. An adequate amount of GDL (0.15 g/L) was added in order to initiate the acid gelation process at 25 °C. 480 μL of Rhodamine B-stained solutions were immediately placed in compartments of LAB-TEK II cells (Thermo Scientific, USA) and incubated at 25 ºC until image obtention. Gels were observed with a 20.0 × objective with a confocal scanning microscope NIKON Eclipse TE-2000-E (Nikon Instruments Inc., Japan). The acquired images (1024×1024 pixel resolution) were stored in tiff format for further analysis.

In order to perform a quantitative analysis, pore size histograms were obtained for each system after thresholding operation with Image J software and Bone J plugin (Abràmoff, Magalhães, & Ram, 2004; Doube et al., 2010).

In order to obtain the texture parameters of the micrographs, a plugin of the Image J software called "Gray Level Co-occurrence Matrix Texture" (version 0.4) was used. Two texture parameters were analyzed: entropy (E) and homogeneity (H). The E parameter is a measure of the gray histogram variability, whereas the H parameter indicates the distribution of the gray levels within the plane of the image, i.e. H is higher when the image contains fewer transitions of gray tonalities (Haralick, 1982).

ACCEPTED MANUSCRIPT

2.5. Texture profile analysis (TPA)

TPA was performed at room temperature in a universal testing machine Multitest 2.5-d (Mecmesin, West Sussex, United Kingdom) coupled to a digital dynamometer (25 N load cell) using a cylindrical stainless steel probe (20 mm diameter). Before tests, gels were prepared in cylindrical containers (45 mm diameter and 30 mm height) at 25 °C. Each sample (by fivefold) was penetrated axially in a single cycle of 50% of compression at a constant rate of 1.0 mm/s. From each resulting force-distance curve, two texture parameters were obtained: firmness (FN, N/mm), as the initial slope of the penetration curve, and fracture force (FF, N), as the force at which the material fractures.

2.6. Water holding capacity (WHC)

Gel samples of approximately 5 g were centrifuged at 2,265 g for 5 min. Gel samples and the water released were weighted in order to calculate the WHC of the gels as a percentage using the following equation: WHC (%) = 100 [(gel weight – serum weight)/gel weight].

2.7. Statistical analysis

All determinations were performed at least in triplicate and results were expressed as mean ± standard deviation. The statistical analysis was performed by analysis of variance (ANOVA) and Tukey test with Sigma Plot software (11.0 trial version). Differences were considered statistically significant at $p < 0.05$.

ACCEPTED MANUSCRIPT

3. Results and discussion

3.1. SPI/TG phase diagram

Fig. 1 shows the phase diagram corresponding to the mixtures of aqueous solutions of SPI and TG in different proportions. The SPI and polysaccharide concentrations of each binary solution correspond to a single point in the phase diagram. One-phase (miscible) samples were represented by an empty symbol, and a full symbol was assigned to the samples that showed turbidity (gray) or visible phase separation (black). These latter samples showed a segregative phase separation due to thermodynamic incompatibility between SPI proteins and TG, where the lower phase is rich in protein while the upper phase is rich in TG.

Fig. 1

The compatibility curve was obtained by a mathematical adjustment using an exponential decay function of two parameters, as reported by Spyropoulos et al. (2010):

$$C_{SPI}\ (g/L) = 0.849 \times e^{-65.8 \times C_{TG}\ (g/L)} \quad (1)$$

3.2. Protein acid gelation

3.2.1. Initial surface charge of SPI proteins

Surface potential is an important factor for determining the magnitude of charged-based colloidal interactions of a particle, most crucially electrostatic repulsion of other like charged particles (Malhotra & Coupland, 2004). Thus, the ζ potential of SPI in SPI/TG mixtures may be used as an indicator of the electrostatic stability of SPI proteins and are shown in Table 1.

Table 1

As expected for proteins with a pI below the isoionic pH, heat-treated SPI solutions prepared in distilled water showed a highly negative potential (Table 1). This negative

ζ potential decreased not only in the presence of TG, but also when TG concentration increased from 0.01 to 0.05 g/L. This decrease in the surface charge of SPI particles could weaken the inter-particle electrostatic repulsion, promoting protein aggregation and further aggregate formation (Song, Zhou, Fu, Chen, & Wu, 2013). This phenomenon should be taken into account in order to evaluate the gelling behavior of SPI in SPI/TG mixtures, as discussed below.

3.2.2. Gel microstructure analysis

Fig. 2 shows the digital images obtained by CLSM for SPI acid gels in the presence and absence of TG. Upon Rhodamine B-staining, protein structures appear in red color while the black areas correspond to gel pores and/or the continuous phase of TG.

Fig. 2

It is important to highlight that the micrographs show remarkable changes in the microstructure, which depend on the TG concentration in the mixture. In the absence of TG (Fig. 2A), SPI gels have a homogenous and compact microstructure with small water-filled pores whose average diameter is (0.872 ± 0.005) μm.

On the other hand, several authors have reported protein/polysaccharide mixed gels with stable phase separated microstructures, e.g., coarse stranded, protein continuous, polysaccharide continuous and bicontinuous ones (Beldengrün et al., 2018; Corredig et al., 2011; Hidalgo et al., 2015; Stieger & van de Velde, 2013; van den Berg, van Vliet, van der Linden, van Boekel, & van de Velde, 2007). These gels consist of mixtures of thermodynamically incompatible biopolymers in aqueous solutions, but there are no previous reports of cold-set gels of SPI/TG mixtures.

For SPI/TG gels, the microstructures observed depended on the concentration of TG added. In the presence of the lowest TG concentration (Fig. 2 B), the protein network

was less interconnected and presented pores with a mean diameter of (2.9 ± 0.2) μm. This value was significantly higher ($p < 0.05$) than the mean diameter obtained for SPI gel systems, i.e., in the absence of TG, as reported above. This microstructure is known as "coarse stranded" since the protein forms a coarse and an isotropic network, uniformly distributed throughout the non-protein phase. When TG was present in 0.02 g/L, the protein network showed no connectivity (Fig. 3C). In this type of microstructure, called "bicontinuous gel", the non-protein phase forms continuous channels through the protein phase (van den Berg et al., 2007).

SPI/TG acidified systems with TG concentrations of 0.03 g/L or more (Fig. 2D, E, and F) showed droplet-shaped structures of protein phase within the continuous TG phase. Interestingly, these droplet-shaped structures increased their average size with TG concentration: (15.6 ± 0.8) μm, (16.4 ± 0.9) μm, and (21.959 ± 0.001) μm for TG concentrations of 0.03, 0.04, and 0.05 g/L, respectively. These microstructures would result from the combination of gelation and segregative phase separation processes. The gradual decrease in the colloidal stability of SPI particles due to the decrease in the negative ζ potential when TG concentration increases (Table 1) may also contribute to this behavior.

The segregative phase separation process might result from depletion interaction linked to repulsion between soy proteins and TG particles. If we consider each protein colloidal particle as a sphere surrounded by a layer of a certain thickness, inaccessible to the galactomannan's center of mass (depletion layer), when other protein particles approach and overlap their depletion layers, the volume of the solution available for the polysaccharide increases (de Bont, van Kempen, & Vreeker, 2002). This phenomenon causes an increase in the entropy and a consequent decrease in the free energy, which in turn causes an attractive interaction between the protein particles, making droplet-

shaped protein inclusions disperse in a continuous phase of TG. Esquena (2016) also considered that this microstructure corresponds to a water-in-water emulsion stabilized due to the formation of gelled states that prevented coalescence. During the gelation process, especially in the presence of high concentrations of a thickening agent like TG, the increase in viscosity causes a decrease in the protein particle movement, and therefore, the phase separation is delayed. In this context, the protein droplets are capable of forming stable colloidal dispersions of microgel particles.

In a similar way, Monteiro et al. (2013) also reported the dependence of the heat-induced gels microstructure on TG concentration. These authors observed gels with a dispersed galactomannan phase in a continuous protein phase in SPI/TG mixed systems at similar concentrations of TG but higher SPI concentrations.

The texture parameters S and H were also calculated from the digital images, whose values as a function of TG concentration are shown in Fig. 3.

Fig. 3

SPI/TG gels with a "bicontinuous" microstructure (0.02 g/L TG) and "polysaccharide continuous" microstructure (≥ 0.03 g/L TG) showed maximum values of H and minimum values of E. As explained before, H is inversely related to the number of transitions of gray tonalities and E is maximal for an image containing the full range of grays with equal probability. Therefore, these results agree with the named microstructures, in which the particles are distributed in such a way that there are few gray transitions (high H values) and small gray histogram variability (low E values). Thus, this H-increase and E-decrease indicate that protein particles are located in well-defined sectors. Particularly for the bicontinuous microstructure to the W/W emulsion transition at TG concentrations of 0.02 and 0.03 g/L, respectively, H decreased significantly ($p < 0.05$). This can be related to the evident increase in the number of

gray tonalities transitions within the plane of the image obtained from the bicontinuous gel SPI/TG system (Fig. 2C) in comparison with the number of gray tonalities transitions within the plane of the image obtained from the droplet-shaped microstructures of protein phase in the W/W emulsion (Fig. 2D). This transition was accompanied with a significant E-increment ($p < 0.05$), due to an increment in the gray histogram variability. Interestingly, for W/W emulsions, this H-decrease and E-increase changed to an inverted tendency when TG increases from 0.03 to 0.05 g/L (Fig. 2E, 2C, and 2F, respectively). In this case, the H-increment with TG concentration can be related to the increment in the size of the droplet-shaped microstructures of protein phase, and to the lower number of these microstructures in the entire CLSM image. Despite the fact that these changes in these W/W emulsions were less evident for E parameter, E decreased significantly with TG concentration, due to the decrease in the gray histogram variability of the corresponded images.

3.2.3. Texture profile analysis

Table 2 summarizes the results obtained from the FN and FF of SPI acid gels in the presence and absence of TG (0, 0.01, 0.03, and 0.05 g/L).

Table 2

In the absence of TG and in the presence of the lowest galactomannan concentration, there were no significant differences in FF values ($p > 0.05$). However, at higher galactomannan concentrations, the FF could not be obtained from the force-distance curves. On the other hand, the FN of gels decreased significantly when TG concentration increased in SPI/TG gels. These findings indicate that the protein gelation process would be affected by the presence of TG, obtaining weaker gels as TG concentration increases. This behavior can be related to the competition between SPI

ACCEPTED MANUSCRIPT

acid gelation and phase separation processes due to the thermodynamic incompatibility between SPI and TG. In the presence of lowest TG concentration, the relative rate between both processes allows the gel mesh formation but reduces the rearrangement of the protein-protein interactions, leading to a gel with lower firmness than SPI ones. As the concentration of TG increases, the formation of W/W emulsions of soy proteins in the galactomannan continuous phase results in the formation of colloidal dispersions of microgel particles instead of an interconnected protein network, leading to an abrupt decrease in gel firmness and to a significant loss of fracture capacity.

3.2.4. Water holding capacity (WHC)

Fig. 4 shows the results of the WHC of SPI gels (0.3 g/L) in the absence and the presence of TG. It is observed that the WHC decreases significantly with the addition of increasing concentrations of TG.

Fig. 4

As mentioned above, an increment in TG concentration in SPI/TG gels promoted significant changes in the microstructure of the protein gel (Fig. 2). As expected, since the presence of increased quantities of TG promoted a gradual disruption of the protein gel network, the gel matrix showed a gradual loss of its capacity to retain the absorbed water, shown as a gradual loss of WHC (Fig. 4).

4. Conclusions

The phase diagram of SPI/TG systems showed a segregative phase separation due to thermodynamic incompatibility between SPI proteins and TG. ζ potential of heat-treated SPI proteins in SPI/TG mixtures revealed an electrostatic stability loss in the presence of TG, which may promote a higher propensity for protein aggregation during the cold-

set gelation upon GDL addition. Also, the microstructural analysis showed remarkable changes in the SPI/TG gelled systems, which depended on the TG concentration present in the mixture. These different microstructures may be attributed to a different balance between gelation and segregative phase separation processes. SPI gels showed a homogenous and compact microstructure. When TG was present, the protein network became less and less interconnected when TG concentration increased (coarse-stranded and bicontinuous gels, respectively). For higher TG concentrations, stable W/W emulsions were formed. Interestingly, the protein droplet-shaped structures in these latest colloidal systems increased in their average sizes when TG concentration increased. A quantitative analysis of the micrographs revealed an H-increase and an E-decrease when TG concentration increased. Finally, TPA showed that all these microstructural changes were related to an abrupt decrease in gel firmness, a significant loss of fracture capacity, and also, to a significant decrease in the water holding capacity.

The findings of this work may be of interest to the food industry since acid gels of soy proteins with different microstructures can be obtained by varying the concentration of TG. Therefore, novel gelled foods with different textures and sensory characteristics can be developed. On the other hand, this study has revealed a simple method for obtaining stable W/W emulsions based in cold-set gelation of aqueous mixtures of heat-treated SPI dispersions and TG. Thus, these colloidal suspensions of microgel particles obtained may also be used to encapsulate bioactive hydrophilic compounds and/or to stabilize natural dyes, broadening the application of these SPI/TG mixed systems.

ACCEPTED MANUSCRIPT

Acknowledgements

This study was financially supported by the Universidad Nacional de Rosario, Argentina (PID 1BIO439), and Consejo Interuniversitario Nacional (CIN)/ Consejo Nacional de Investigaciones Científicas y Técnicas (CONICET) (PDTS 196). We would like to thank the staff from the English Department of the Facultad de Ciencias Bioquímicas y Farmacéuticas (UNR) for the language correction of the manuscript. Romina Ingrassia is a research awardee of CONICET.

5. References

Abràmoff, M. D., Magalhães, P. J., & Ram, S. J. (2004). Image processing with ImageJ. *Biophotonics international, 11*(7), 36-42.

Alting, A. C., de Jongh, H. H. J., Visschers, R. W., & Simons, J.-W. F. A. (2002). Physical and Chemical Interactions in Cold Gelation of Food Proteins. *Journal of Agricultural and Food Chemistry, 50*(16), 4682-4689.

Ananthakumar, R., Chitra, K., & Satheshkumar, S. (2018). A review on applications of natural polymers in gastroretentive drug delivery system. *Drug Invention Today, 10*, 285-289.

Anderson, E. (1949). Endosperm mucilages of legumes. Occurrence and composition. *Industrial and Engineering Chemistry 41*(12), 2887-2890.

Anema, S. G., & Klostermeyer, H. (1996). ζ-Potentials of casein micelles from reconstituted skim milk heated at 120 °C. *International Dairy Journal, 6*(7), 673-687.

Beldengrün, Y., Aragon, J., Prazeres, S. F., Montalvo, G., Miras, J., & Esquena, J. (2018). Gelatin/Maltodextrin Water-in-Water (W/W) Emulsions for the

Preparation of Cross-Linked Enzyme-Loaded Microgels. *Langmuir, 34*(33), 9731-9743.

Buffington, L. A., Stevens, E. S., Morris, E. R., & Rees, D. A. (1980). Vacuum ultraviolet circular dichroism of galactomannans. *International Journal of Biological Macromolecules, 2*(4), 199-203.

Campbell, L. J., Gu, X., Dewar, S. J., & Euston, S. R. (2009). Effects of heat treatment and glucono-[delta]-lactone-induced acidification on characteristics of soy protein isolate. *Food Hydrocolloids, 23*(2), 344-351.

Corredig, M., Sharafbafi, N., & Kristo, E. (2011). Polysaccharide–protein interactions in dairy matrices, control and design of structures. *Food Hydrocolloids, 25*(8), 1833-1841.

Daas, P. J. H., Grolle, K., van Vliet, T., Schols, H. A., & de Jongh, H. H. J. (2002). Toward the Recognition of Structure−Function Relationships in Galactomannans. *Journal of Agricultural and Food Chemistry, 50*(15), 4282-4289.

de Bont, P. W., van Kempen, G. M. P., & Vreeker, R. (2002). Phase separation in milk protein and amylopectin mixtures. *Food Hydrocolloids, 16*(2), 127-138.

de Kruif, C. G. (1997). Skim Milk Acidification. *Journal of Colloid and Interface Science, 185*(1), 19-25.

Doube, M., Kłosowski, M. M., Arganda-Carreras, I., Cordelières, F. P., Dougherty, R. P., Jackson, J. S. (2010). BoneJ: Free and extensible bone image analysis in ImageJ. *Bone, 47*(6), 1076-1079.

Doublier, J. L., Garnier, C., Renard, D., & Sanchez, C. (2000). Protein-polysaccharide interactions. *Current Opinion in Colloid & Interface Science, 5*(3-4), 202-214.

ACCEPTED MANUSCRIPT

Esquena, J. (2016). Water-in-water (W/W) emulsions. *Current Opinion in Colloid & Interface Science, 25*, 109-119.

Friedman, M., & Brandon, D. L. (2001). Nutritional and health benefits of soy proteins. *Journal of Agricultural and Food Chemistry, 49*, 1069-1086.

Goswami, S., & Naik, S. (2014). Natural gums and its pharmaceutical application. *Journal of Scientific and Innovative Research, 3*(1), 112-121.

Grinberg, V. Y., & Tolstoguzov, V. B. (1997). Thermodynamic incompatibility of proteins and polysaccharides in solutions. *Food Hydrocolloids, 11*(2), 145-158.

Gu, X., Campbell, L. J., & Euston, S. R. (2009). Influence of sugars on the characteristics of glucono-[delta]-lactone-induced soy protein isolate gels. *Food Hydrocolloids, 23*(2), 314-326.

Haralick, R. M. (1982). Image texture survey. In E. P.R. Krishnaiah and L.N. Kanal (Ed.), *Handbook of Statistics* (pp. 399-415): Elsevier.

Hidalgo, M., Fontana, M., Armendariz, M., Riquelme, B., Wagner, J., & Risso, P. (2015). Acid-Induced Aggregation and Gelation of Sodium Caseinate-Guar Gum Mixtures. *Food Biophysics, 10*(2), 181-194.

Jóźwiak, B., Dziubiński, M., & Orczykowska, M. (2018). Wettability of commercial starches and galactomannans. [Article]. *Journal of Dispersion Science and Technology, 39*(8), 1085-1092.

Kasapis, S. (2008). Phase separation in biopolymer gels: a low- to high-solid exploration of structural morphology and functionality. *Critical Reviews in Food Science and Nutrition, 48*(4), 341-359.

Khan, R. S., Nickerson, M. T., Paulson, A. T., & Rousseau, D. (2011). Release of fluorescent markers from phase-separated gelatin-maltodextrin hydrogels. *Journal of Applied Polymer Science, 121*(5), 2662-2673.

ACCEPTED MANUSCRIPT

Lundin, L., Norton, I., Foster, T., Williams, M., Hermansson, A., & Bergström, E. (1999). Phase separation in mixed biopolymer systems. In P. Williams & G. Phillips (Eds.), *10th International gums and stabilizers for the food industry: the past, present and future of food hydrocolloids* (pp. 167–180). Cambridge, UK: Woodhead Publishing

Malhotra, A., & Coupland, J. N. (2004). The effect of surfactants on the solubility, zeta potential, and viscosity of soy protein isolates. *Food Hydrocolloids, 18*(1), 101-108.

Monteiro, S. R., Rebelo, S., da Cruz e Silva, O. A. B., & Lopes-da-Silva, J. A. (2013). The influence of galactomannans with different amount of galactose side chains on the gelation of soy proteins at neutral pH. *Food Hydrocolloids, 33*(2), 349-360.

Moure, A., Sineiro, J., Domínguez, H., & Parajó, J. C. (2006). Functionality of oilseed protein products: A review. *Food Research International, 39*(9), 945-963.

Nkonge, C., & Ballance, G. M. (1982). A sensitive colorimetric procedure for nitrogen determination in micro-Kjeldahl digests. *Journal of Agricultural and Food Chemistry, 30*(3), 416-420.

Norton, I. T., & Frith, W. J. (2001). Microstructure design in mixed biopolymer composites. *Food Hydrocolloids, 15*(4-6), 543-553.

Singh, S., Singh, G., & Arya, S. K. (2018). Mannans: An overview of properties and application in food products. *International Journal of Biological Macromolecules, 119*, 79-95.

Song, X., Zhou, C., Fu, F., Chen, Z., & Wu, Q. (2013). Effect of high-pressure homogenization on particle size and film properties of soy protein isolate. *Industrial Crops and Products, 43*, 538-544.

ACCEPTED MANUSCRIPT

Sorgentini, D. A., & Wagner, J. R. (1999). Comparative study of structural characteristics and thermal behavior of whey and isolate soybean proteins. *Journal of Food Biochemistry, 23*(5), 489-507.

Spyropoulos, F., Portsch, A., & Norton, I. T. (2010). Effect of sucrose on the phase and flow behaviour of polysaccharide/protein aqueous two-phase systems. *Food Hydrocolloids, 24*(2-3), 217–226.

Stieger, M., & van de Velde, F. (2013). Microstructure, texture and oral processing: New ways to reduce sugar and salt in foods. *Current Opinion in Colloid & Interface Science, 18*(4), 334-348.

Tavares, C., Monteiro, S. R., Moreno, N., & Lopes da Silva, J. A. (2005). Does the branching degree of galactomannans influence their effect on whey protein gelation? *Colloids and Surfaces A: Physicochemical and Engineering Aspects, 270–271*(0), 213-219.

Tolstoguzov, V. (2003). Some thermodynamic considerations in food formulation. *Food Hydrocolloids, 17*(1), 1-23.

van den Berg, L., van Vliet, T., van der Linden, E., van Boekel, M. A. J. S., & van de Velde, F. (2007). Breakdown properties and sensory perception of whey proteins/polysaccharide mixed gels as a function of microstructure. *Food Hydrocolloids, 21*(5-6), 961-976.

Wu, Y., Ding, W., & He, Q. (2018). The gelation properties of tara gum blended with κ-carrageenan or xanthan. *Food Hydrocolloids, 77*, 764-771.

Xiao, C. W. (2011). 22 - Functional soy products. In M. Saarela (Ed.), *Functional Foods (Second edition)* (pp. 534-556): Woodhead Publishing.

ACCEPTED MANUSCRIPT

ACCEPTED MANUSCRIPT

Figure captions

Fig. 1. Phase diagram of SPI/GT mixtures in buffer phosphate 10 mM pH 7, after 48 h at 25 °C: (●) two-phase samples; (○) one-phase clear solution; (●) one-phase turbid solution.

Fig. 2. Digital images obtained by CLSM of SPI acid gels without (A) and with different TG concentrations: (B) 0.01 g/L, (C) 0.02 g/L, (D) 0.03 g/L, (E) 0.04 g/L and (F) 0.05 g/L; SPI 0.3 g/L; GDL 0.15 g/L; temperature = 25 °C; objective zoom = 40x. White bars correspond to 100 μm.

Fig. 3. Textural parameters obtained from the digital images of SPI acid gels in the presence and the absence of TG: Entropy E (A) and Homogeneity H (B). SPI 0.3 g/L; GT 0 - 0.05 g/L, GDL 0.15 g/L; temperature = 25 °C.

Fig. 4. Water holding capacity (WHC) as a function of TG concentration. SPI 0.3 g/L, GDL 0.15 g/L; temperature = 25 °C.

ACCEPTED MANUSCRIPT

ACCEPTED MANUSCRIPT

Table 1. Electrokinetic potential of heat-treated SPI (0.3 g/L) at different TG concentrations.

C_{TG} (g/L)	ζ potential (mV)
-	-29.54 ± 2.10[a]
0.01	-23.98 ± 1.25[b]
0.02	-20.90 ± 3.49[b,c]
0.03	-17.34 ± 2.36[c,d]
0.04	-14.32 ± 1.69[d]
0.05	-13.40 ± 0.67[d]

*Mean value ± standard deviation (n=5). Means within the same column following by different letters are significantly different ($p < 0.05$).

ACCEPTED MANUSCRIPT

ACCEPTED MANUSCRIPT

Table 2. Firmness (FN) and Fracture Force (FF) obtained from force (N) vs. distance (mm) curves of 0.3 g/L SPI acid gels and SPI/TG acid gels at different TG concentrations (0.15 g/L GDL).

C_{TG} (g/L)	FN (N/mm)	FF (N)
0	$0.8 \pm 0.2^{a,*}$	0.33 ± 0.02^{a}
0.01	0.09 ± 0.02^{b}	0.35 ± 0.03^{a}
0.03	0.04 ± 0.01^{c}	N/A†
0.05	0.0068 ± 0.0001^{d}	N/A

*Mean value ± standard deviation (n=5). Means within the same column following by different letters are significantly different ($p < 0.05$). †N/A = not applicable.

ACCEPTED MANUSCRIPT

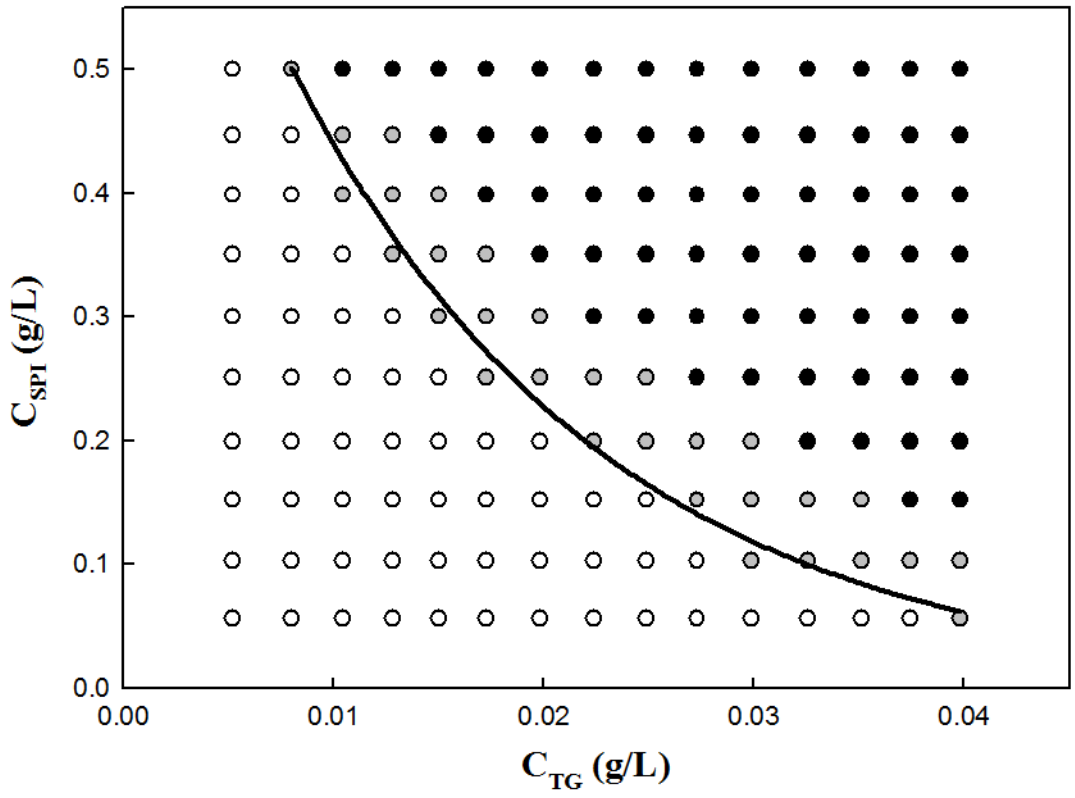

ACCEPTED

ACCEPTED MANUSCRIPT

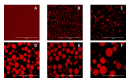

ACCEPTED MANUSCRIPT

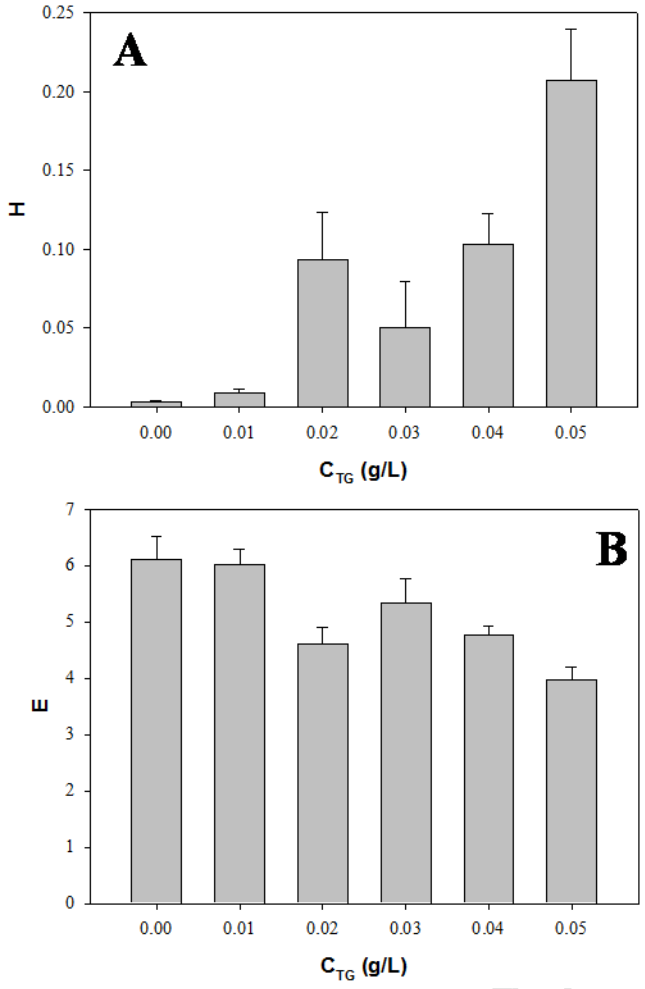

ACCEPTED MANUSCRIPT

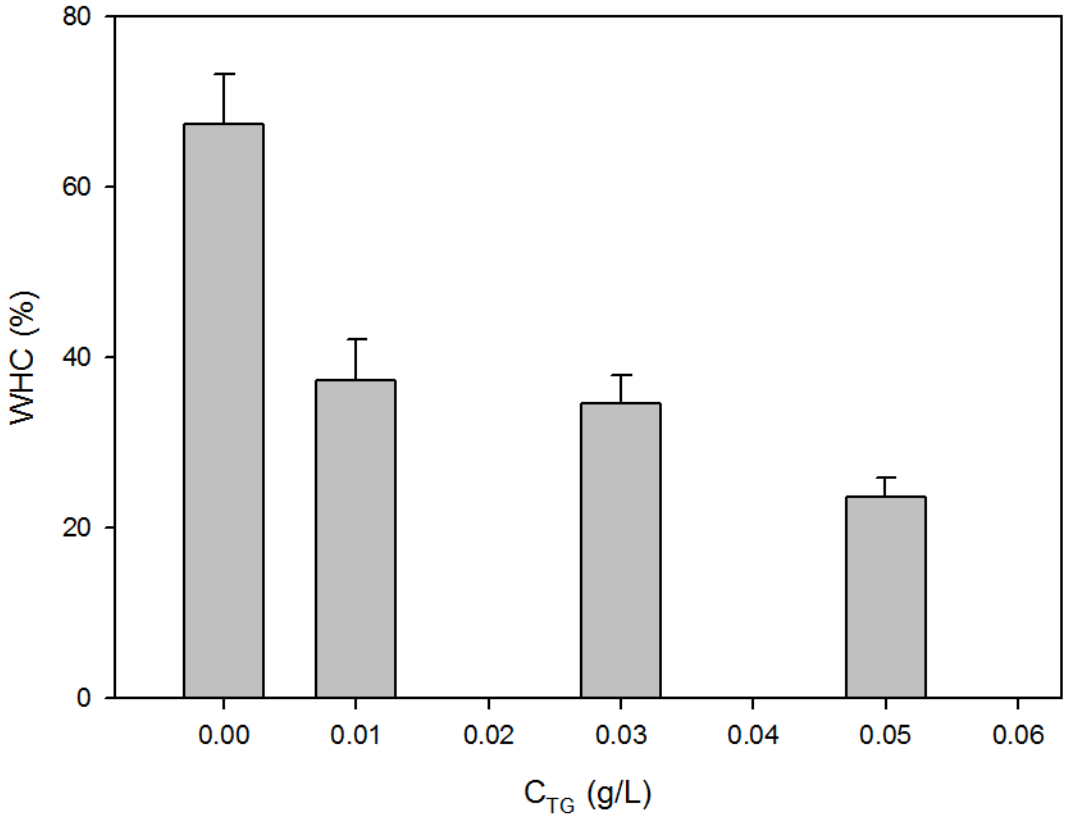

ACCEPTED

ACCEPTED MANUSCRIPT

- Soy protein isolate/tara gum gels showed substantially different microstructures.
- Different cold-set gel microstructures were related to different texture behavior.
- The gel firmness decrease occurred along with its water holding capacity.
- This study has revealed a simple method for obtaining stable W/W emulsions.

ACCEPTED MANUSCRIPT